Cell Biol Toxicol (2010) 26:421–434
DOI 10.1007/s10565-010-9153-7

Transcriptional and posttranscriptional regulation of CYP1A1 by vanadium in human hepatoma HepG2 cells

Ghada Abdelhamid · Anwar Anwar-Mohamed · Osama A. Badary · Adel A. Moustafa · Ayman O.S. El-Kadi

Received: 16 October 2009 / Accepted: 5 February 2010 / Published online: 11 March 2010

Abstract We recently demonstrated that V^{5+} downregulates 2,3,7,8-tetrachlorodibenzo-*p*-dioxin (TCDD)-mediated induction of Cyp1a1 mRNA, protein, and catalytic activity levels in Hepa 1c1c7 cells through transcriptional mechanism. Therefore, it is important to investigate whether similar changes occur in humans. For this purpose, we examined the effect of V^{5+} (as ammonium metavanadate, NH_4VO_3) on the expression of aryl hydrocarbon receptor (AhR)-regulated gene; cytochrome P450 1A1 (CYP1A1) at each step of the AhR signal transduction pathway in human hepatoma HepG2 cells. Our results show a significant reduction in TCDD-mediated induction of CYP1A1 mRNA, protein, and activity levels after V^{5+} treatment in a dose-dependent manner. Investigating the effect of co-exposure to V^{5+} and TCDD at transcriptional levels revealed that V^{5+} significantly inhibited TCDD-mediated induction of AhR-dependent luciferase reporter gene expression. Looking at the posttranscriptional level, V^{5+} did not affect CYP1A1 mRNA stability, thus eliminating the possible role of V^{5+} in modifying CYP1A1 gene expression through this mechanism. On the other hand, at the posttranslational level, V^{5+} was able to significantly decrease CYP1A1 protein half-life contributing to the inconsistency between catalytic activity and transcriptional level. Importantly, we showed that V^{5+} did not significantly alter the heme oxygenase-1 mRNA level, thus eliminating any possibility that V^{5+} might have decreased CYP1A1 activity through affecting its heme content. This study demonstrates for the first time that V^{5+} downregulates the expression of CYP1A1 at the transcriptional, posttranscriptional and posttranslational mechanisms in the human hepatoma HepG2 cells.

Keywords Aryl hydrocarbon receptor · Cytochrome P450 1A1 · Vanadium · Carcinogenesis

Electronic supplementary material The online version of this article (doi:10.1007/s10565-010-9153-7) contains supplementary material, which is available to authorized users.

G. Abdelhamid · A. Anwar-Mohamed · A. O. El-Kadi (✉)
Faculty of Pharmacy & Pharmaceutical Sciences,
3126 Dentistry/Pharmacy Centre, University of Alberta,
Edmonton, Alberta, Canada T6G 2N8
e-mail: aelkadi@pharmacy.ualberta.ca

O. A. Badary
Department of Clinical Pharmacy, Faculty of Pharmacy,
Ain Shams University,
Cairo, Egypt

G. Abdelhamid · A. A. Moustafa
Department of Pharmacology and Toxicology,
Faculty of Pharmacy, Helwan University,
Helwan, Egypt

Introduction

The aryl hydrocarbon receptor (AhR) is a ligand-activated cytoplasmic transcription factor that belongs to the basic-helix–loop-helix protein family (Lubet et al. 1984). In the absence of a ligand, AhR is associated

with two 90-kDa heat shock protein-90, the 23-kDa heat shock protein, and hepatitis B virus X-associated protein 2. Following ligand binding, AhR translocates to the nucleus, dissociates from the complex, and forms a heterodimer with the AhR nuclear translocator (Arnt) (Hankinson 1995). The whole complex then acts as a transcription factor that binds to a specific DNA recognition sequence, termed the xenobiotic responsive element (XRE), located in the promoter region of a number of AhR-regulated genes. Among these genes, cytochrome P450 1A1 (CYP1A1) is the most capable of bioactivating the toxic and environmental contaminants polycyclic aromatic hydrocarbons (PAHs) and halogenated aromatic hydrocarbons (HAHs) to carcinogenic metabolites (Denison and Nagy 2003). Of interest, it has been shown that the toxicological effects of PAHs and the more toxic HAHs, typified by 2,3,7,8-tetrachlorodibenzo-*p*-dioxin (TCDD), are mainly mediated through the activation of AhR and consequently CYP1A1. In fact, a well-established link between the induction of CYP1A1 and cancer has been previously reported (McLemore et al. 1990).

The toxicological effects of individual AhR ligands have been extensively studied; yet, the combined toxicological effects of these ligands with heavy metals such as vanadium (V^{5+}) are currently at large. V^{5+} compounds exert protective effects against chemical-induced carcinogenesis in animals, by modifying various xenobiotic enzymes, thus, inhibiting carcinogen-derived active metabolites generation. The anticarcinogenic effects of V^{5+} combined with its low toxicity have made V^{5+} an attractive tool for the treatment of different cancers. Moreover, recent studies have suggested V^{5+} as an effective non-platinum metal antitumor agent (Kostova 2009). The major difference between platinum anticancer agents and V^{5+} is that the former react with nitrogen atoms of DNA and preferentially react with the N-7 atom of deoxyguanylic acid (Knox et al. 1986). This type of DNA damage produced by platinum anticancer agents is thought to be the major reason for their effectiveness (Rosenberg et al. 1969). On the contrary, V^{5+} is believed to mediate its anticancer effect mainly through three different mechanisms: firstly by inactivating the carcinogens-generating metabolizing enzymes such as CYP1A1, secondly through affecting cell proliferation, and lastly, through inducing cellular oxidative stress (Evangelou 2002).

To date, very little information is available on the effect of V^{5+} on the CYP1A1 expression and function (Anwar-Mohamed and El-Kadi 2008). As such, we have previously demonstrated that V^{5+} was able to decrease the TCDD-mediated induction of Cyp1a1 at mRNA, protein, and catalytic activity levels in the mouse hepatoma, Hepa 1c1c7 cells (Anwar-Mohamed and El-Kadi 2008). Therefore, the objectives of the current study were to examine the effect of co-exposure to V^{5+} and TCDD on the expression of human CYP1A1 using human hepatoma HepG2 cells and to investigate the underlying mechanisms involved in this modulation. The human hepatoma cell line HepG2 cells offers a good model to examine the effect of V^{5+} on the TCDD-mediated induction of CYP1A1 for the following reasons: (1) the AhR is widely expressed in all mouse tissues (Abbott and Probst 1995; Abbott et al. 1995), while in humans, this expression is only high in lungs, thymus, liver, and kidneys (Puga et al. 2009); (2) these cells have proven to be a useful model for investigating the regulation of human CYP1A1 (Lipp et al. 1992; Krusekopf et al. 1997; Kikuchi et al. 1996; Kim et al. 2006; Vakharia et al. 2001); (3) human hepatocytes have been shown to be one of major targets for heavy metals (Ercal et al. 2001); (4) compared to primary human hepatocytes, HepG2 cells are relatively easy-to-handle tool to study the regulation of CYP1A1 (Westerink and Schoonen 2007).

We provide here the first evidence that V^{5+} downregulates human CYP1A1 expression at transcriptional level and posttranscriptional levels.

Materials and methods

Materials

Ammonium metavanadate (NH_4VO_3), 3-(4,5-dimethylthiazol-2-yl)-2,5-diphenyltetrazolium bromide (MTT), cycloheximide (CHX), 7-ethoxyresorufin, and protease inhibitor cocktail were purchased from Sigma–Aldrich (St. Louis, MO). 2,3,7,8-Tetrachlorodibenzo-*p*-dioxin, >99% pure, was purchased from Cambridge Isotope Laboratories (Woburn, MA). TRIzol reagent and Lipofectamine 2000 reagents were purchased from Invitrogen (San Diego, CA). The High-Capacity cDNA Reverse Transcription Kit and SYBR Green PCR Master Mix were purchased from

Applied Biosystems (Foster City, CA). Actinomycin-D (Act-D) was purchased from Calbiochem (San Diego, CA). Chemiluminescence Western blotting detection reagents were from GE Healthcare Life Sciences (Piscataway, NJ). Nitrocellulose membrane was purchased from Bio-Rad (Hercules, CA). CYP1A1 D-15 mouse anti-rat polyclonal primary antibody was purchased from Santa Cruz Biotechnology, Inc. (Santa Cruz, CA), anti-mouse IgG peroxidase secondary antibody was purchased from R&D Systems (Minneapolis, MN, USA). pRL-CMV plasmid and luciferase assay reagents were obtained from Promega (Madison, WI). All other chemicals were purchased from Thermo Fisher Scientific (Toronto, ON, Canada). Primers were purchased from Integrated DNA Technologies, Inc. (Coralville, IA) and are listed in Table 1.

Cell culture

Human hepatoma HepG2 cell line, ATCC number HB-8065 (Manassas, VA), passages 4–15, was maintained in Dulbecco's modified Eagle's medium supplemented with 10% heat-inactivated fetal bovine serum and 1% penicillin–streptomycin. Cells were grown in 75-cm^2 cell culture flasks at 37°C in a 5% CO_2 humidified incubator.

Chemical treatments

Cells were treated in serum-free medium with various concentrations of V^{5+} (25–1,000 μM) in the absence and presence of 1 nM TCDD as described in figure legends. TCDD was dissolved in dimethyl sulfoxide (DMSO) and maintained in DMSO at −20°C until use. V^{5+} was prepared freshly in double-deionized water (10 mM stock). In all treatments, the DMSO concentration did not exceed 0.05% (*v*/*v*).

Table 1 Primers sequences used for real-time PCRs

Gene	Forward primer	Reverse primer
CYP1A1	5′-CTA TCT GGG CTG TGG GCA A-3′	5′-CTG GCT CAA GCA CAA CTT GG-3′
HO-1	5′-ATG GCC TCC CTG TAC CAC ATC-3′	5′-TGT TGC GCT CAA TCT CCT CCT-3′
β-actin	5′-CTG GCA CCC AGC ACA ATG-3′	5′-GCC GAT CCA CAC GGA GTA CT-3′

Effect of V^{5+} on cell viability

The effect of V^{5+} on cell viability was determined using the MTT assay as described previously (Anwar-Mohamed and El-Kadi 2009b). MTT assay measures the conversion of MTT to formazan in living cells via mitochondrial enzymes of viable cells. In brief, HepG2 cells were seeded onto 96-well microtiter cell culture plates and incubated for 24 h at 37°C in a 5% CO_2 humidified incubator. Cells were treated with various concentrations of V^{5+} (25–1,000 μM) in the absence and presence of 1 nM TCDD. After 24 h incubation, the medium was removed and replaced with cell culture medium containing 1.2 mM MTT dissolved in phosphate-buffered saline (PBS, pH 7.4). After 2 h of incubation, the formed crystals were dissolved in isopropanol. The intensity of the color in each well was measured at a wavelength of 550 nm using the Bio-Tek EL 312e microplate reader (Bio-Tek Instruments, Winooski, VT).

RNA extraction and cDNA synthesis

Total RNA was isolated using TRIzol reagent (Invitrogen) according to the manufacturer's instructions and quantified by measuring the absorbance at 260 nm. Thereafter, first-strand cDNA synthesis was performed by using the high-capacity cDNA reverse transcription kit (Applied Biosystems) according to the manufacturer's instructions. Briefly, 1.5 μg of total RNA from each sample was added to a mix of 2.0 μl 10× RT buffer, 0.8 μl 25× dNTP mix (100 mM), 2.0 μl 10× RT random primers, 1.0 μl MultiScribe™ reverse transcriptase, and 3.2 μl nuclease-free water. The final reaction mix was kept at 25°C for 10 min, heated to 37°C for 120 min, heated for 85°C for 5 s, and finally cooled to 4°C.

Quantification by real-time PCR

Quantitative analysis of specific mRNA expression was performed by real-time PCR, by subjecting the resulting cDNA to PCR amplification using 96-well optical reaction plates in the ABI Prism 7500 System (Applied Biosystems). Twenty-five-microliter reaction mix contained 0.1 μl of 10 μM forward primer and 0.1 μl of 10 μM reverse primer (40 nM final concentration of each primer), 12.5 μl of SYBR Green Universal Mastermix, 11.05 μl of nuclease-free

water, and 1.25 µl of cDNA sample. The primers used in the current study were chosen from previously published studies (Song and Freedman 2005; Rushworth and MacEwan 2008; Cho et al. 2006) and are listed in Table 1. Assay controls were incorporated onto the same plate, namely, no-template controls to test for the contamination of any assay reagents. After sealing the plate with an optical adhesive cover, the thermocycling conditions were initiated at 95°C for 10 min, followed by 40 PCR cycles of denaturation at 95°C for 15 s, and anneal/extension at 60°C for 1 min. Melting curve (dissociation stage) was performed by the end of each cycle to ascertain the specificity of the primers and the purity of the final PCR product.

Real-time PCR data analysis

The real-time PCR data were analyzed using the relative gene expression, i.e., ($\Delta\Delta C_T$) method as described in Applied Biosystems User Bulletin No. 2 and explained further by Livak and Schmittgen (2001). In brief, the primers used in the current study were tested to avoid primer dimers, self-priming formation, or unspecific amplification. To ensure the quality of the measurements, each plate included, for each gene, a negative control and a positive control. For each sample, a threshold cycle (C_T) was calculated based on the time (measured by the number of PCR cycles) at which the reporter fluorescent emission increased beyond a threshold level (based on the background fluorescence of the system). The triplicate measurements for each sample were averaged to give an average C_T value for each group, after removing of outliers (Oscar Aparicio et al. 2005). The samples were diluted in such a manner that the C_T value was observed between 15 and 30 cycles. Results were expressed using the comparative C_T method as described in User Bulletin 2 (Applied Biosystems). Briefly, the ΔC_T values were calculated in every sample for each gene of interest as follows: $C_{T\ \text{gene of interest}} - C_{T\ \text{reporter gene}}$, with β-actin as the reporter gene. Calculation of relative changes in the expression level of one specific gene ($\Delta\Delta C_T$) was performed by subtraction of ΔC_T of control (untreated cells or 0 h time point) from the ΔC_T of the corresponding treatment groups. The values and ranges given in different figures were determined as follows: $2^{-\Delta\Delta CT}$ with $\Delta\Delta C_T + SE$ and $\Delta\Delta C_T - SE$, where SE is the standard error of the mean of the $\Delta\Delta C_T$ value (User Bulletin 2, Applied Biosystems).

Protein extraction and Western blot analysis

Twenty-four hours after incubation with the test compounds, cells were collected in lysis buffer containing 50 mM HEPES, 0.5 M sodium chloride, 1.5 mM magnesium chloride, 1 mM EDTA, 10% (*v*/*v*) glycerol, 1% Triton X-100, and 5 µl/ml of protease inhibitor cocktail. The cell homogenates were obtained by incubating the cell lysates on ice for 1 h, with intermittent vortexing every 10 min, followed by centrifugation at 12,000×*g* for 10 min at 4°C. The supernatant fractions were collected for determination of protein concentration using bovine serum albumin as a standard by the Lowry method (Gebremedhin et al. 2000). Proteins (50 µg) were resolved by denaturing electrophoresis, as described previously (Anwar-Mohamed and El-Kadi 2008). Briefly, the cell homogenates were dissolved in 1x sample buffer, boiled for 5 min, separated by 10% SDS-PAGE, and electrophoretically transferred to a nitrocellulose membrane. Protein blots were blocked for 24 h at 4°C in blocking buffer containing 5% skim milk powder, 2% bovine serum albumin, and 0.05% (*v*/*v*) Tween 20 in Tris-buffered saline solution (0.15 M sodium chloride, 3 mM potassium chloride, and 25 mM Tris base). After blocking, the blots were incubated with a CYP1A1 primary antibody for 4 h at room temperature in Tris-buffered saline containing 0.05% (*v*/*v*) Tween 20 and 0.02% sodium azide. Incubation with a peroxidase-conjugated anti-mouse IgG secondary antibody for CYP1A1 was carried out in blocking buffer for 1 h at room temperature. The bands were visualized with the enhanced chemiluminescence method according to the manufacturer's instructions (GE Healthcare, Mississauga, ON). The intensity of CYP1A1 protein bands was quantified relative to the signals obtained for GAPDH protein, using ImageJ image processing program (National Institutes of Health, Bethesda, MD, http://rsb.info.nih.gov/ij).

Determination of CYP1A1 enzymatic activity

CYP1A1-dependent 7-ethoxyresorufin *O*-deethylase (EROD) activity was performed on intact, living cells using 7-ethoxyresorufin as a substrate, as previously

described (Elbekai and El-Kadi 2004). Enzymatic activity was normalized to cellular protein content, which was determined using a modified fluorescent assay (Lorenzen and Kennedy 1993).

Transient transfection and luciferase assay

HepG2 cells were plated onto 12-well cell culture plates. XRE-driven luciferase reporter plasmid pGudLuc 6.1 and the renilla luciferase pRL-CMV vector, used for normalization, were co-transfected into HepG2 cells. Each well of cells was transfected with 1.5 μg of pGudLuc 6.1 (generously provided by Dr. Michael S. Denison, University of California, Davis, CA) and 0.1 μg pRL-CMV using Lipofectamine 2000 reagent according to the manufacturer's instructions (Invitrogen). The luciferase assay was performed according to the manufacturer's instructions (Promega). In brief, after incubation with test compounds for 24 h, cells were washed with PBS, 200 μl of Passive Lysis Buffer (Promega) was added into each well with continuous shaking for at least 20 min, and then the content of each well was collected separately in 1.5-ml microcentrifuge tubes. Enzyme activities were determined using a Dual-Luciferase reporter assay system (Promega). Quantification was performed using a TD-20/20 luminometer (Turner BioSystems, Sunnyvale, CA).

CYP1A1 mRNA stability

The half-life of CYP1A1 mRNA was determined by an Act-D chase assay. Cells were pretreated with 1 nM TCDD for 12 h. Thereafter, cells were then washed three times and incubated with 5 μg/ml Act-D to inhibit further RNA synthesis, immediately before treatment with 100 μM V^{5+}. Total RNA was extracted at 0, 1, 3, 6, 12, and 24 h after incubation with V^{5+}. Real-time PCRs were performed using SYBR Green PCR Master Mix. The fold change in the level of CYP1A1 (target gene) between treated and untreated cells, corrected by the level of β-actin, was determined using the following equation: Fold change= $2^{-\Delta\ (\Delta CT)}$, where $\Delta C_T = C_{T\ (target)} - C_{T\ (ß\text{-}actin)}$ and $\Delta(\Delta C_T) = \Delta C_{T(treated)} - \Delta C_{T(untreated)}$.

CYP1A1 protein stability

The half-life of CYP1A1 protein was analyzed by the CHX chase assay. Cells were pretreated with 1 nM TCDD for 24 h. Thereafter, cells were then washed three times and incubated with 10 μg/ml CHX to inhibit further protein synthesis, immediately before treatment with 100 μM V^{5+}. Cell homogenates were extracted at 0, 1, 3, 6, 12, and 24 h after incubation with V^{5+}. Cellular protein was determined using the method of Lowry et al. (1951). CYP1A1 protein was measured by Western blotting. The intensity of CYP1A1 protein bands was quantified relative to the signals obtained for GAPDH protein, using ImageJ software. The protein half-life values were determined from semilog plots of integrated densities versus time.

Statistical analysis

The comparative analysis of the results from various experimental groups with their corresponding controls was performed using SigmaStat for Windows (Systat Software, Inc., San Jose, CA). A one-way analysis of variance followed by the Student–Newman–Keul test was carried out to assess statistical significance. For dose-dependency significance, *t* test between different V^{5+} treatments was performed. The differences were considered significant when $P<0.05$.

Results

Effect of co-exposure to V^{5+} and TCDD on cell viability

To determine the maximum nontoxic concentrations of V^{5+} to be utilized in the current study, HepG2 cells were treated for 24 h with increasing concentrations of V^{5+} (25–1,000 μM) in the absence and presence of 1 nM TCDD. Thereafter, cytotoxicity was measured using MTT assay. Figure 1 shows that V^{5+} alone at the concentrations of 25 to 250 μM did not affect cell viability. However, the highest concentration tested, 1,000 μM, significantly decreased cell viability to approximately 57%. Similarly, co-exposure to V^{5+} and TCDD caused a significant decrease in cell viability, only at the highest concentration tested (1,000 μM), to approximately 52% (Fig. 1).

Time-dependent effect of co-exposure to V^{5+} and TCDD on CYP1A1 mRNA

To better understand the kinetics of CYP1A1 mRNA in response to the co-exposure to V^{5+} and TCDD, the

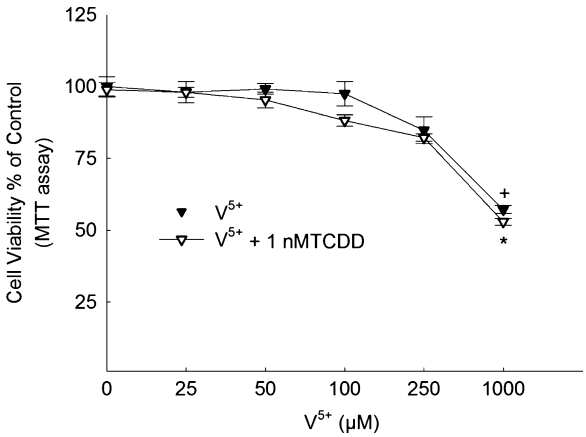

Fig. 1 Effect of V^{5+} on cell viability. HepG2 cells were treated for 24 h with V^{5+} (0, 25, 50, 100, 250, and 1,000 μM) in the absence and presence of 1 nM TCDD. Cell cytotoxicity was determined using MTT. Data are expressed as percentage of untreated control (which is set at 100%)±SE (n=8). +P<0.05, compared with control (concentration=0 μM); *P<0.05, compared with the respective TCDD (T) treatment

time-dependent effect was determined at various time points up to 24 h after treatment with 1 nM TCDD in the absence and presence of 100 μM V^{5+} (Fig. 2). Our results clearly demonstrated that TCDD alone caused a time-dependent increase in CYP1A1 mRNA levels and reached a maximum induction at 24 h to reach 3500%. In contrast, when HepG2 cells were co-exposed to V^{5+} and TCDD, there was a significant decrease in the CYP1A1 mRNA levels that occurred as early as 3 h by 39% compared to TCDD alone. Similarly, there was a statistically significant decrease in the TCDD-mediated induction of CYP1A1 mRNA levels in response to V^{5+} treatment at 6, 12, and 24 h by 49%, 63%, and 91%, respectively, compared to TCDD alone (Fig. 2).

Concentration-dependent effect of co-exposure to V^{5+} and TCDD on CYP1A1 mRNA

To examine the effect of co-exposure to V^{5+} and TCDD on CYP1A1 mRNA, HepG2 cells were treated with various concentrations of V^{5+} in the presence of 1 nM TCDD (Fig. 3). Thereafter, CYP1A1 mRNA was assessed using real-time PCR. TCDD alone caused 1600% increase in CYP1A1 mRNA that was inhibited in a dose-dependent manner by V^{5+}. Initially, V^{5+} at the concentration of 25 μM caused a significant decrease in the TCDD-mediated induction of CYP1A1 mRNA by 12%. The maximum inhibi-

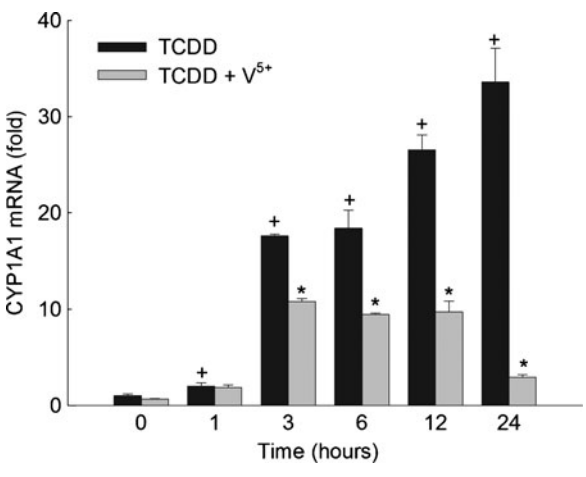

Fig. 2 Time-dependent effect of V^{5+} on CYP1A1 mRNA. HepG2 cells were treated with 1 nM TCDD in the absence and presence of V^{5+} (100 μM). First-strand cDNA was synthesized from total RNA (1 μg) extracted from HepG2 cells. cDNA fragments were amplified and quantitated using an ABI 7500 real-time PCR system as described under "Materials and methods." Duplicate reactions were performed for each experiment, and the values presented are the means of three independent experiments. *P<0.05, compared with the respective TCDD treatment; +P<0.05, compared with control (zero time)

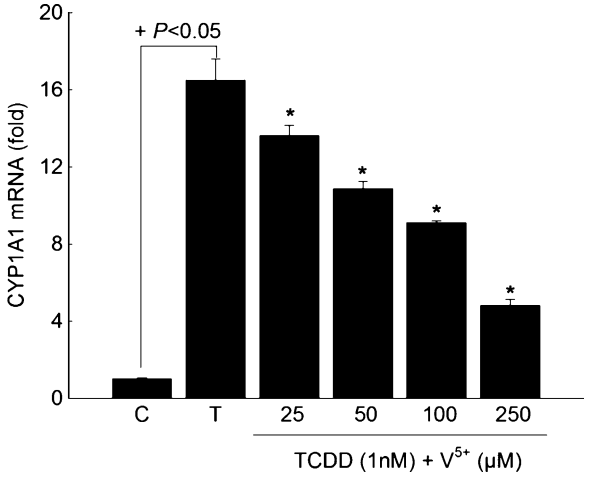

Fig. 3 Concentration-dependent effect of V^{5+} on CYP1A1 mRNA. HepG2 cells were treated for 6 h with increasing concentrations of V^{5+} in the presence of 1 nM TCDD. First-strand cDNA was synthesized from total RNA (1 μg) extracted from HepG2 cells. cDNA fragments were amplified and quantitated using an ABI 7500 real-time PCR system as described under "Materials and methods." Duplicate reactions were performed for each experiment, and the values presented are the means of three independent experiments. +P<0.05, compared with control (C) (concentration=0 μM); *P<0.05, compared with the respective TCDD (T) treatment

tion took place at the highest concentration tested, 250 μM, by 71% compared to TCDD alone (Fig. 3).

Concentration-dependent effect of co-exposure to V^{5+} and TCDD on CYP1A1 protein and catalytic activity

To investigate whether the observed inhibition of the TCDD-mediated induction of CYP1A1 mRNA is reflected at the protein and activity levels, HepG2 cells were treated for 24 h with 1 nM TCDD in the absence and presence of increasing concentrations of V^{5+}. Figure 4a and b shows that TCDD alone caused 3200% and 3900% increase in CYP1A1 protein and catalytic activity levels, respectively. On the other hand, V^{5+} significantly reduced the TCDD-mediated induction of CYP1A1 protein and catalytic activity levels (Fig. 4a and b). V^{5+} decreased CYP1A1 protein in a dose-dependent manner while causing further inhibition to CYP1A1 catalytic activity levels starting at V^{5+} concentration of 25 μM and reached the plateau at 50 μM (Fig. 4a and b). CYP1A1 protein was decreased by 22%, 48%, 63%, and 81% with V^{5+} concentrations of 25, 50, 100, and 250 μM, respectively (Fig. 4a). On the other hand, CYP1A1 activity was decreased by 70%, 81%, 85%, and 87% with V^{5+} concentrations of 25, 50, 100, and 250 μM, respectively (Fig. 4b).

Transcriptional inhibition of *CYP1A1* gene by V^{5+}

To determine if the observed effect upon co-exposure to V^{5+} and TCDD on CYP1A1 is occurring through an AhR-dependent mechanism, HepG2 cells were transiently co-transfected with the XRE-driven luciferase reporter gene and its control construct, renilla luciferase. Luciferase activity results showed that 100 μM V^{5+} alone did not alter the luciferase activity (Fig. 5). TCDD alone (1 nM) was capable of causing a significant induction of the luciferase activity by 1100%, as compared with control. On the other hand, co-treatment with V^{5+} and TCDD significantly decreased the luciferase activity by more than 75% compared to TCDD alone (Fig. 5).

Posttranscriptional modification of CYP1A1 mRNA by V^{5+}

The level of mRNA expression is a function of the transcription rate, and the elimination rate, through

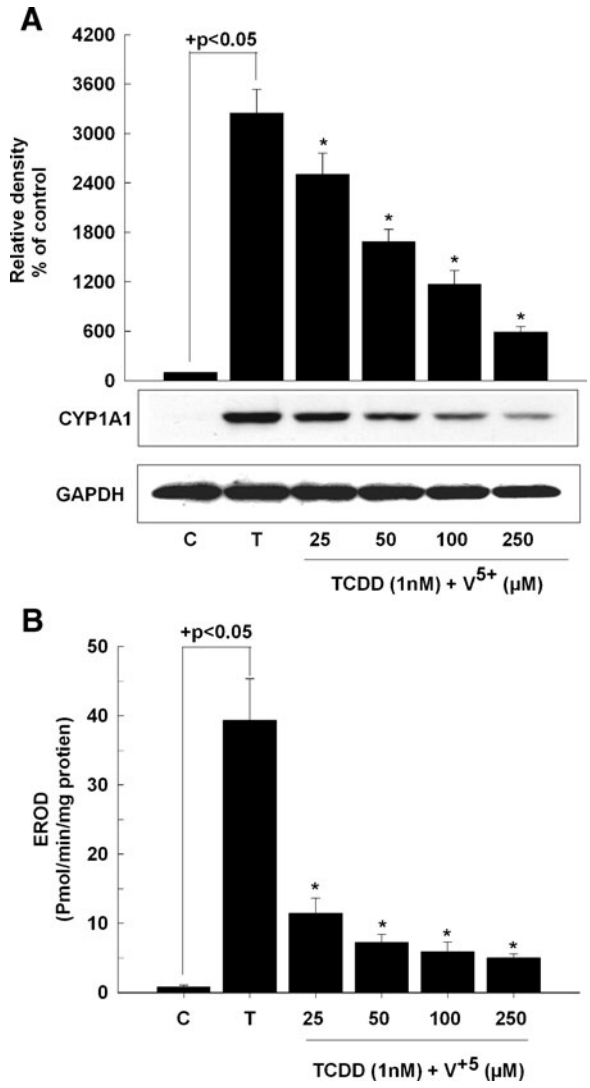

Fig. 4 Effect of V^{5+} on inducible CYP1A1 protein and catalytic activity. HepG2 cells were treated for 24 h with increasing concentrations of V^{5+} in the presence of 1 nM TCDD. **a** Microsomal protein (50 μg) was separated by 10% SDS-PAGE and transferred to a nitrocellulose membrane. Protein blots were then blocked overnight at 4°C and incubated with a primary CYP1A1/1A2 antibody for 4 h at 4°C, followed by 1 h incubation with secondary antibody at room temperature. CYP1A1 protein was detected using the enhanced chemiluminescence method. The intensity of bands was normalized to GAPDH signals, which was used as a loading control. One of three representative experiments is shown. **b** CYP1A1 activity was measured in intact living cells treated with increasing concentrations of V^{5+}, in the absence and presence of 1 nM TCDD for 24 h. CYP1A1 activity was measured using 7-ethoxyresorufin as a substrate. Values are presented as mean ± S.E. (n=8). +P<0.05, compared with control (C); *P<0.05, compared with the respective TCDD (T) treatment

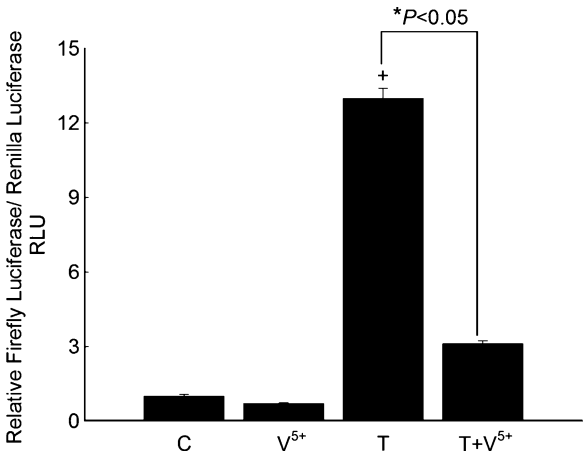

Fig. 5 Effect of V^{5+} on AhR-dependent luciferase activity. HepG2 cells were transiently co-transfected with the XRE-luciferase transporter plasmid pGudLuc 6.1 and renilla luciferase control plasmid pRL-CMV. Cells were treated with vehicle, TCDD (1 nM), V^{5+} (100 μM), or TCDD (1 nM)+V^{5+} (100 μM) for 24 h. Thereafter, cells were lysed, and luciferase activity was measured according to the manufacturer's instruction. Luciferase activity is reported as relative light units (*RLU*). Values are presented as mean ± SE (n=4). +P<0.05, compared with control (*C*); *P<0.05, compared with the respective TCDD (*T*) treatment

processing or degradation. Therefore, we examined the effect of V^{5+} on the stability of human CYP1A1 mRNA transcripts, using an Act-D chase experiment. Our results showed that CYP1A1 mRNA is a short-lived mRNA with a half-life of 4.52±0.22 h (Fig. 6). On the other hand, co-exposure to V^{5+} and TCDD did not significantly alter the CYP1A1 mRNA level compared with TCDD alone, indicating that the decrease in CYP1A1 mRNA transcripts in response to V^{5+} was not due to any increase in its degradation.

Posttranslational modification of CYP1A1 Protein by V^{5+}

The fact that V^{5+} inhibited TCDD-mediated induction of CYP1A1 catalytic activity much more than what is observed at the mRNA levels raised the question of whether V^{5+} could modify CYP1A1 protein stability. Therefore, the effect of V^{5+} on CYP1A1 protein half-life was determined using CHX chase experiment. Figure 7 shows that CYP1A1 protein induced by TCDD degraded with a half-life of 8.26±0.37 h. Interestingly, V^{5+} significantly decreased the stability of CYP1A1 protein which degraded with a half-life of 5.38±0.12 h (Fig. 7).

Effect of co-exposure to V^{5+} and TCDD on HO-1 mRNA

In the current study, we examined the effect of V^{5+} on HO-1 mRNA, a rate-limiting enzyme of heme degradation. For this purpose, HepG2 cells were treated with increasing concentrations of V^{5+} (25–

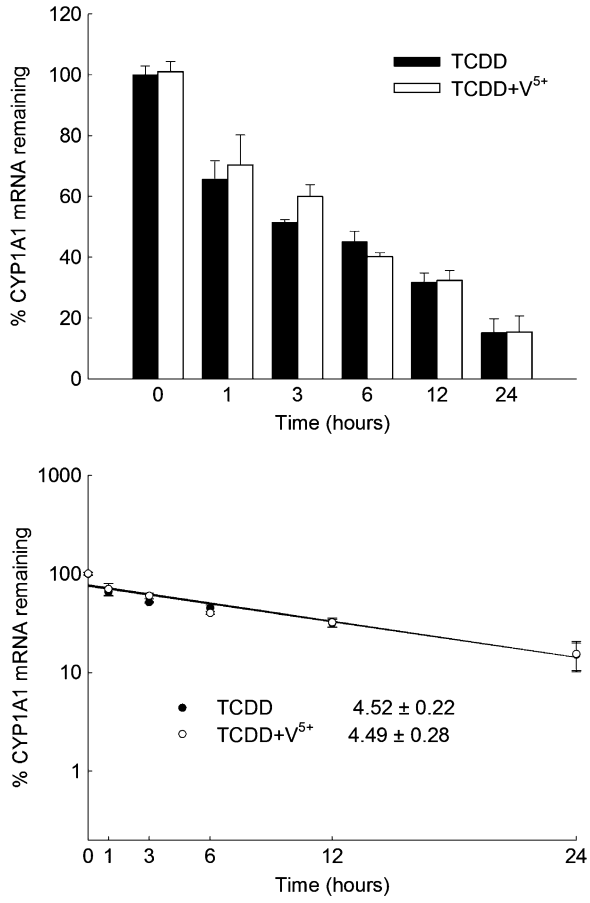

Fig. 6 Effect of V^{5+} on CYP1A1 mRNA half-life. HepG2 cells were grown to 90% confluence in six-well cell culture plates and were treated with 1 nM TCDD for 12 h. The cells were then washed three times and incubated in fresh media containing 100 μM V^{5+} plus 5 μg/ml Act-D, a RNA synthesis inhibitor. First-strand cDNA was synthesized from total RNA (1.5 μg) extracted from HepG2 cells. cDNA fragments were amplified and quantitated using an ABI 7500 real-time PCR system as described under "Materials and methods." mRNA decay curves were analyzed individually, and the half-life was estimated from the slope of a straight line fitted by linear regression analysis to a semilog plot of mRNA amount, expressed as a percentage of treatment at time=0 h (maximum, 100%) level, versus time. The half-lives obtained from three independent experiments were then used to calculate the mean half-life (mean ± SE, n=3)

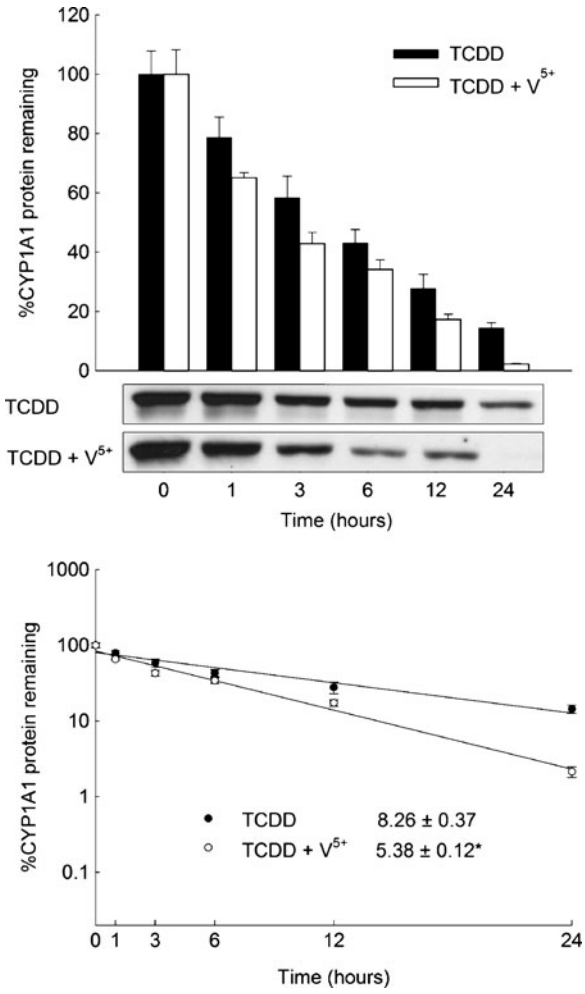

Fig. 7 Effect of V^{5+} on the CYP1A1 protein half-life. HepG2 cells were grown to 90% confluence in six-well cell culture plates. Thereafter, the cells were treated with 1 nM TCDD for 24 h. Cells were washed and incubated in fresh media containing 100 μM V^{5+} plus 10 μg/ml CHX, a protein translation inhibitor. Microsomal protein was extracted at the designated time points after the addition of CHX. Protein (50 μg) was separated by 10% SDS-PAGE and transferred to a nitrocellulose membrane. The intensities of CYP1A1 protein bands were normalized to GAPDH signals, which were used as loading controls. All protein decay curves were analyzed individually. The half-life was estimated from the slope of a straight line fitted by linear regression analysis to a semilog plot of protein amount, expressed as a percentage of treatment at time=0 h (maximum, 100%) level, versus time. The half-lives obtained from three independent experiments were then used to calculate the mean half-life (mean ± SE, n=3). *p<0.05 compared with TCDD

250 μM) in the presence of 1 nM TCDD. Thereafter, HO-1 mRNA was measured using real-time PCR. Figure 8 shows that TCDD alone did not alter HO-1 mRNA level. Similarly, co-exposure to TCDD and V^{5+} did not significantly alter the HO-1 mRNA level. Thus, HO-1 is not involved in the V^{5+}-mediated decrease in the TCDD-mediated induction of CYP1A1 catalytic activity.

Direct effect of V^{5+} on TCDD-mediated induction of CYP1A1 catalytic activity

To examine the possible direct inhibitory effect of V^{5+} on CYP1A1 catalytic activity, HepG2 cells were treated for 24 h with 1 nM TCDD. Thereafter, cells were incubated with increasing concentrations of V^{5+} for 2 h, and the CYP1A1 catalytic activity levels were determined in intact living cells using EROD assay. Our results showed that TCDD alone significantly increased CYP1A1 catalytic activity, by 4000%. In contrast, V^{5+} did not cause a direct inhibitory effect on the TCDD-mediated induction of CYP1A1 catalytic activity levels (Fig. 9).

Discussion

AhR ligands such as TCDD occur as by-products in the manufacture of organochlorides, in the incineration of chlorine-containing substances such as

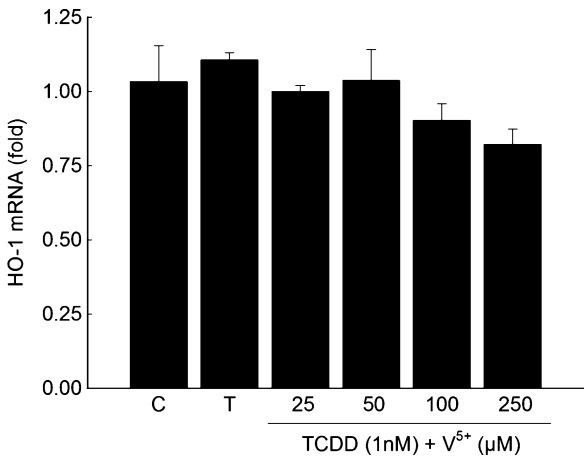

Fig. 8 Effect of V^{5+} on HO-1 mRNA. HepG2 cells were treated for 6 h with increasing concentrations of V^{5+} in the presence of 1 nM TCDD. First-strand cDNA was synthesized from total RNA (1.5 μg) extracted from HepG2 cells. cDNA fragments were amplified and quantitated using ABI 7500 real-time PCR system as described under "Materials and methods." Duplicate reactions were performed for each experiment, and the values presented are the means of three independent experiments

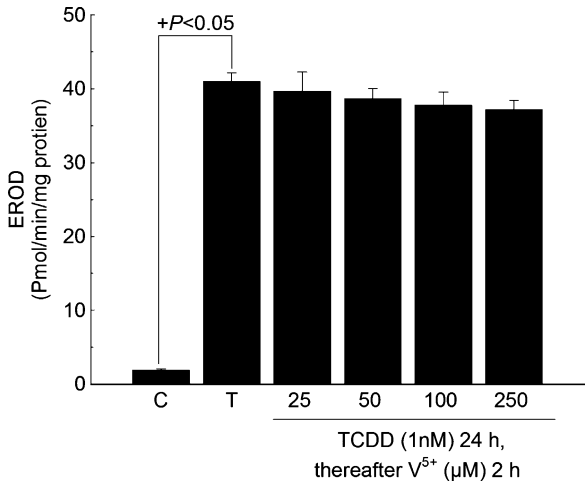

Fig. 9 Direct effect of V^{5+} on inducible CYP1A1 activity. HepG2 cells were treated for 24 h with 1 nM TCDD and then cells were incubated with 100 μM V^{5+} for additional 2 h. Thereafter, CYP1A1 activity was measured using 7-ethoxyresorufin as a substrate. Values are presented as mean ± S.E. (n=8). +P<0.05, compared with control (C)

polyvinyl chloride, in the bleaching of paper, and from natural sources such as volcanoes and forest fires (Weber et al. 2008). The main route of human contamination seems to be through the food (Svensson et al. 1991). TCDD is a stable hydrophobic contaminant which persists in the environment (Skene et al. 1989). This feature of TCDD is responsible for its accumulation in the food and its sustained effects on animal and human health (Schuetz et al. 1995; Stapleton and Baker 2003).

Environmental contamination by vanadium has dramatically increased during the last decades, especially in the most developed countries due to the widespread use of fossil fuels, many of which liberate fine particulates of V^{5+} to the atmosphere during combustion (Baran 2008). Humans consume appreciable amounts of V^{5+} in food and water (Evangelou 2002). The estimated daily intake of V^{5+} is 10 to 60 μg (Nechay 1984). In addition, the highest level of V^{5+} supplements in multivitamin products reaches 25 μg/tablet or capsule. Furthermore, weight training athletes are reported to use up to 18.6 mg V^{5+} per day as a body-building supplement (Barceloux 1999). An estimate of the total body pool of vanadium in healthy individuals is 100 to 200 μg (Haiman et al. 2003). If we take into consideration the fact that heavy metals such as V^{5+} are significantly deposited in hepatocytes and kidneys (Edel and Sabbioni 1989), the concentrations used in the current study are of great relevance to those in humans.

During the last few years, V^{5+} compounds have been shown to be effective in inhibiting cancers of the liver (Bishayee and Chatterjee 1995), lung, breast, and gastrointestinal tract (Kopf-Maier 1987; Kanna et al. 2004). The mechanism for this anticancer effect is not known. However, previous studies have demonstrated that V^{5+} compounds exert protective effects against chemical-induced carcinogenesis mainly by modifying various xenobiotic-metabolizing enzymes (Evangelou 2002). Data from our laboratory and others showed that heavy metals other than V^{5+} are capable of modifying the carcinogen-metabolizing enzyme, Cyp1a1, at different stages of its regulatory pathway (Bessette et al. 2005; Khan et al. 2007; Korashy and El-Kadi 2008).

Previous studies have shown that inhibition of TCDD-mediated induction of CYP1A1 might be, in part, through inducing cell cycle arrest which will subsequently inhibit the AhR transcriptional activity in G2/M phase of the cell cycle (Santini et al. 2001). In contrast, other studies have shown that arsenic (As^{3+}) inhibition of the TCDD-mediated induction of CYP1A1 is independent of cell cycle arrest but may involve other mechanisms such as the recruitment of RNA polymerase II (Bonzo et al. 2005). Biphasic effects of vanadium compounds (ammonium metavanadate, vanadyl sulfate trihydrate, and ortho-sodium vanadate) on cell cycle arrest have also been reported on in vitro tumor colony growth models. In these studies, it was shown that V^{5+} salts at low ($<10^{-10}$ M) concentrations stimulated, and at higher ($>10^{-10}$ M) concentrations inhibited, colony formation in human tumors (Hanauske et al. 1987). Thus, one of the mechanisms that might have been involved in the V^{5+} inhibition of the TCDD-mediated induction of CYP1A1 is through inducing cell cycle arrest; however, this hypothesis is yet to be confirmed.

In the current study, we hypothesize that V^{5+} protects against TCDD-mediated toxicity and carcinogenicity by inhibiting CYP1A1 gene expression. Hence, the main objective of the current study was to determine the potential effects of co-exposure to V^{5+} and TCDD on the expression of CYP1A1. We have shown previously that V^{5+} downregulates the Cyp1a1 gene expression in murine Hepa 1c1c7 through a transcriptional mechanism. Thus, we initially examined the effect of V^{5+} on the expression of CYP1A1

mRNA in human HepG2 cells. In the current study, we showed that V^{5+} inhibits the TCDD-mediated induction of CYP1A1 mRNA in a concentration-dependent manner. To determine if the inhibition of CYP1A1 mRNA is further reflected at the protein and catalytic activity levels, we measured the effect of V^{5+} on CYP1A1 protein and catalytic activity levels. Our results showed that V^{5+} inhibits CYP1A1 protein in a dose-dependent manner while causing further inhibitory effect at the activity level as the level of inhibition reached plateau at 50 μM. In agreement with our results, we have shown previously that V^{5+} down-regulates Cyp1a1 gene expression in a concentration-dependent manner in murine Hepa 1c1c7 cells at the mRNA, protein as well as activity levels (Anwar-Mohamed and El-Kadi 2008).

We have reported previously that heavy metals modulate Cyp1a1 through transcriptional, posttranscriptional, and posttranslational mechanisms (Korashy and El-Kadi 2005; Elbekai and El-Kadi 2007). Thus, it was of great importance to examine the effect of V^{5+} on the transcriptional and posttranscriptional regulation of CYP1A1. The cellular mRNA level at any time point is a function of the rate of its production, through a transcriptional mechanism, and the rate of its degradation. In the current study, we demonstrated that co-exposure to V^{5+} (100 μM) and TCDD inhibited CYP1A1 mRNA expression in a time-dependent manner, with a maximum inhibition at 24 h. Therefore, it is apparent that V^{5+} inhibits CYP1A1 mRNA by decreasing the *de novo* synthesis.

To confirm that the effect of V^{5+} on CYP1A1 gene expression is mediated through an AhR-dependent mechanism, luciferase reporter gene assay was carried out. Our results showed that V^{5+} inhibited the TCDD-mediated induction of the XRE-dependent luciferase activity. Thus, the downregulation of CYP1A1 gene expression by V^{5+} was mediated through an AhR-dependent mechanism. The mechanisms controlling AhR functions and homeostasis include several protein kinases that modulate AhR subcellular localization, transcriptional activity, and protein stability. The three families of mitogen-activated protein kinases (MAPKs), extracellular signal-regulated kinases, c-Jun N-terminal/stress-activated protein kinases, and the p38s are important intracellular signal transduction mediators involved in the control of gene expression and various other events in eukaryotic cells through the phosphorylation of transcription factors and the modulation of their function (Henklova et al. 2008; Puga et al. 2009). In this regard, it has been shown that V^{5+} is a potent activator of MAPKs (Samet et al. 1998). Therefore, the observed effect of V^{5+} on CYP1A1 might be due to two possible mechanisms. Firstly, V^{5+} activates the p38 MAPK and subsequently induces the transcription of nuclear transcription factor-κB (NF-κB), a factor involved in CYP1A1 inhibition (Jaspers et al. 2000; Chen et al. 1999). Secondly, it has been well documented that cytosolic AhR requires phosphorylation prior to ligand binding; thus, it might have been that V^{5+} through inducing MAPK inhibited the phosphorylation of AhR with a subsequent inhibition to its ATP-dependent nuclear translocation (Wang and Safe 1994).

To examine whether V^{5+} inhibited CYP1A1 mRNA through decreasing its stability, the half-life of the CYP1A1 mRNA was determined by an Act-D chase experiment. Our results demonstrated that V^{5+} did not affect CYP1A1 mRNA stability, suggesting that V^{5+} did not have a posttranscriptional modulating effect on the expression of CYP1A1 mRNA, which is similar to the result that has been obtained with Hepa 1c1c7 (Anwar-Mohamed and El-Kadi 2008).

The effect of V^{5+} on the CYP1A1 catalytic activity level suggests the presence of a posttranslational mechanism. For this purpose, we examined the effect of V^{5+} on CYP1A1 protein stability, HO-1 mRNA, and the possible competition between V^{5+} and the CYP1A1 substrate, 7-ethoxyresorufin. At the protein stability level, our results showed that V^{5+} significantly decreased the CYP1A1 protein half-life by 35% compared to TCDD alone. The discrepancy between the effect of V^{5+} on CYP1A1 protein expression and its catalytic activity can be explained by the fact that the latter is the sum of action of V^{5+} on CYP1A1 gene expression that was reflected at the protein level (Fig. 4A), in addition to decreasing CYP1A1 protein stability by V^{5+} (Fig. 7). In contrary to our results, we have previously shown in Hepa 1c1c7 cells that V^{5+} did not alter the Cyp1a1 protein stability (Anwar-Mohamed and El-Kadi 2008). These results suggest that the effect of V^{5+} on CYP1A1 is species-specific.

In the current study, we showed that V^{5+} did not significantly alter the HO-1 mRNA level at all concentrations tested, excluding the possibility that V^{5+} might decrease the CYP1A1 activity through affecting its heme content. This result is in agreement

with our previous study which showed that V^{5+} did not significantly alter the HO-1 mRNA level in Hepa 1c1c7. Furthermore, V^{5+} did not directly affect the CYP1A1 activity, suggesting that competitive inhibitory mechanism was not involved in the modulation of CYP1A1 activity by V^{5+}. Although V^{5+} failed to induce HO-1 which has been shown to be induced through the redox-sensitive transcription factor nuclear factor-erythroid 2 p45-related factor 2/antioxidant responsive element pathway (Anwar-Mohamed and El-Kadi 2009a), V^{5+} was found to induce the expression of hypoxia inducible factor 1 alpha (HIF-1α) and vascular endothelial growth factor through the phosphatidylinositol 3-kinase/Akt pathway and reactive oxygen species (Gao et al. 2002). Since HIF-1α and AhR share the same transcription factor, Arnt for hypoxia- and AhR-mediated signaling pathways, respectively, we might suggest that hypoxia inhibits TCDD-mediated induction of CYP1A1 expression due to the competition between HIF-1α and the AhR for Arnt (Kim and Sheen 2000).

In conclusion, the present study demonstrates that V^{5+} downregulates the bioactivating enzyme, CYP1A1 in human HepG2 cells through transcriptional and posttranscriptional mechanisms. However, further studies are needed to investigate the cytoprotective effect of V^{5+} against TCDD-mediated toxicity.

Acknowledgments This work was supported by Natural Sciences and Engineering Research Council of Canada (NSERC) Discovery Grant RGPIN 250139-07 to A.O.S. G.A. is the recipient of Egyptian government Scholarship award. A.A-M. is the recipient of Alberta Ingenuity Graduate Scholarship award.

References

Abbott BD, Probst MR. Developmental expression of two members of a new class of transcription factors: II. Expression of aryl hydrocarbon receptor nuclear translocator in the C57BL/6 N mouse embryo. Dev Dyn. 1995;204:144–55.

Abbott BD, Birnbaum LS, Perdew GH. Developmental expression of two members of a new class of transcription factors: I. Expression of aryl hydrocarbon receptor in the C57BL/6 N mouse embryo. Dev Dyn. 1995;204:133–43.

Anwar-Mohamed A, El-Kadi AO. Down-regulation of the carcinogen-metabolizing enzyme cytochrome P450 1a1 by vanadium. Drug Metab Dispos. 2008;36:1819–27.

Anwar-Mohamed A, El-Kadi AO. Down-regulation of the detoxifying enzyme NAD(P)H:quinone oxidoreductase 1 by vanadium in Hepa 1c1c7 cells. Toxicol Appl Pharmacol. 2009a;236:261–9.

Anwar-Mohamed A, El-Kadi AO. Sulforaphane induces CYP1A1 mRNA, protein, and catalytic activity levels via an AhR-dependent pathway in murine hepatoma Hepa 1c1c7 and human HepG2 cells. Cancer Lett. 2009b;275:93–101.

Baran EJ. Vanadium detoxification: chemical and biochemical aspects. Chem Biodivers. 2008;5:1475–84.

Barceloux DG. Vanadium. J Toxicol Clin Toxicol. 1999;37:265–78.

Bessette EE, Fasco MJ, Pentecost BT, Kaminsky LS. Mechanisms of arsenite-mediated decreases in benzo[k]fluoranthene-induced human cytochrome P4501A1 levels in HepG2 cells. Drug Metab Dispos. 2005;33:312–20.

Bishayee A, Chatterjee M. Inhibitory effect of vanadium on rat liver carcinogenesis initiated with diethylnitrosamine and promoted by phenobarbital. Br J Cancer. 1995;71:1214–20.

Bonzo JA, Chen S, Galijatovic A, Tukey RH. Arsenite inhibition of CYP1A1 induction by 2, 3, 7, 8-tetrachlorodibenzo-p-dioxin is independent of cell cycle arrest. Mol Pharmacol. 2005;67:1247–56.

Chen F, Demers LM, Vallyathan V, Ding M, Lu Y, Castranova V, et al. Vanadate induction of NF-kappaB involves IkappaB kinase beta and SAPK/ERK kinase 1 in macrophages. J Biol Chem. 1999;274:20307–12.

Cho SJ, Drechsler H, Burke RC, Arens MQ, Powderly W, Davidson NO. APOBEC3F and APOBEC3G mRNA levels do not correlate with human immunodeficiency virus type 1 plasma viremia or CD4+ T-cell count. J Virol. 2006;80:2069–72.

Denison MS, Nagy SR. Activation of the aryl hydrocarbon receptor by structurally diverse exogenous and endogenous chemicals. Annu Rev Pharmacol Toxicol. 2003;43:309–34.

Edel J, Sabbioni E. Vanadium transport across placenta and milk of rats to the fetus and newborn. Biol Trace Elem Res. 1989;22:265–75.

Elbekai RH, El-Kadi AO. Modulation of aryl hydrocarbon receptor-regulated gene expression by arsenite, cadmium, and chromium. Toxicology. 2004;202:249–69.

Elbekai RH, El-Kadi AO. Transcriptional activation and posttranscriptional modification of Cyp1a1 by arsenite, cadmium, and chromium. Toxicol Lett. 2007;172:106–19.

Ercal N, Gurer-Orhan H, Aykin-Burns N. Toxic metals and oxidative stress part I: mechanisms involved in metal-induced oxidative damage. Curr Top Med Chem. 2001;1:529–39.

Evangelou AM. Vanadium in cancer treatment. Crit Rev Oncol Hematol. 2002;42:249–65.

Gao N, Ding M, Zheng JZ, Zhang Z, Leonard SS, Liu KJ, et al. Vanadate-induced expression of hypoxia-inducible factor 1 alpha and vascular endothelial growth factor through phosphatidylinositol 3-kinase/Akt pathway and reactive oxygen species. J Biol Chem. 2002;277:31963–71.

Gebremedhin D, Lange AR, Lowry TF, Taheri MR, Birks EK, Hudetz AG, et al. Production of 20-HETE and its role in autoregulation of cerebral blood flow. Circ Res. 2000;87:60–5.

Haiman CA, Hankinson SE, De Vivo I, Guillemette C, Ishibe N, Hunter DJ, et al. Polymorphisms in steroid hormone pathway genes and mammographic density. Breast Cancer Res Treat. 2003;77:27–36.

Hanauske U, Hanauske AR, Marshall MH, Muggia VA, Von Hoff DD. Biphasic effect of vanadium salts on in vitro tumor colony growth. Int J Cell Cloning. 1987;5:170–8.

Hankinson O. The aryl hydrocarbon receptor complex. Annu Rev Pharmacol Toxicol. 1995;35:307–40.

Henklova P, Vrzal R, Ulrichova J, Dvorak Z. Role of mitogen-activated protein kinases in aryl hydrocarbon receptor signaling. Chem Biol Interact. 2008;172:93–104.

Jaspers I, Samet JM, Erzurum S, Reed W. Vanadium-induced kappaB-dependent transcription depends upon peroxide-induced activation of the p38 mitogen-activated protein kinase. Am J Respir Cell Mol Biol. 2000;23:95–102.

Kanna PS, Mahendrakumar CB, Indira BN, Srivastawa S, Kalaiselvi K, Elayaraja T, et al. Chemopreventive effects of vanadium toward 1, 2-dimethylhydrazine-induced genotoxicity and preneoplastic lesions in rat colon. Environ Mol Mutagen. 2004;44:113–8.

Khan S, Liu S, Stoner M, Safe S. Cobaltous chloride and hypoxia inhibit aryl hydrocarbon receptor-mediated responses in breast cancer cells. Toxicol Appl Pharmacol. 2007;223:28–38.

Kikuchi H, Kato H, Mizuno M, Hossain A, Ikawa S, Miyazaki J, et al. Differences in inducibility of CYP1A1-mRNA by benzimidazole compounds between human and mouse cells: evidences of a human-specific signal transduction pathway for CYP1A1 induction. Arch Biochem Biophys. 1996;334:235–40.

Kim JE, Sheen YY. Inhibition of 2, 3, 7, 8-tetrachlorodibenzo-p-dioxin (TCDD)-stimulated Cyp1a1 promoter activity by hypoxic agents. Biochem Pharmacol. 2000;59:1549–56.

Kim WK, In YJ, Kim JH, Cho HJ, Kim JH, Kang S, et al. Quantitative relationship of dioxin-responsive gene expression to dioxin response element in Hep3B and HepG2 human hepatocarcinoma cell lines. Toxicol Lett. 2006; 165:174–81.

Knox RJ, Friedlos F, Lydall DA, Roberts JJ. Mechanism of cytotoxicity of anticancer platinum drugs: evidence that cis-diamminedichloroplatinum(II) and cis-diammine-(1, 1-cyclobutanedicarboxylato)platinum(II) differ only in the kinetics of their interaction with DNA. Cancer Res. 1986;46:1972–9.

Kopf-Maier P. Cytostatic non-platinum metal complexes: new perspectives for the treatment of cancer? Naturwissenschaften. 1987;74:374–82.

Korashy HM, El-Kadi AO. Regulatory mechanisms modulating the expression of cytochrome P450 1A1 gene by heavy metals. Toxicol Sci. 2005;88:39–51.

Korashy HM, El-Kadi AO. Modulation of TCDD-mediated induction of cytochrome P450 1A1 by mercury, lead, and copper in human HepG2 cell line. Toxicol In Vitro. 2008;22:154–8.

Kostova I. Titanium and vanadium complexes as anticancer agents. Anticancer Agents Med Chem. 2009;9:827–42.

Krusekopf S, Kleeberg U, Hildebrandt AG, Ruckpaul K. Effects of benzimidazole derivatives on cytochrome P450 1A1 expression in a human hepatoma cell line. Xenobiotica. 1997;27:1–9.

Lipp HP, Schrenk D, Wiesmuller T, Hagenmaier H, Bock KW. Assessment of biological activities of mixtures of polychlorinated dibenzo-p-dioxins (PCDDs) and their constituents in human HepG2 cells. Arch Toxicol. 1992;66:220–3.

Livak KJ, Schmittgen TD. Analysis of relative gene expression data using real-time quantitative PCR and the 2(-Delta Delta C(T)) Method. Methods. 2001;25:402–8.

Lorenzen A, Kennedy SW. A fluorescence-based protein assay for use with a microplate reader. Anal Biochem. 1993;214:346–8.

Lowry OH, Rosebrough NJ, Farr AL, Randall RJ. Protein measurement with the Folin phenol reagent. J Biol Chem. 1951;193:265–75.

Lubet RA, Brunda MJ, Taramelli D, Dansie D, Nebert DW, Kouri RE. Induction of immunotoxicity by polycyclic hydrocarbons: role of the Ah locus. Arch Toxicol. 1984; 56:18–24.

Mclemore TL, Adelberg S, Liu MC, Mcmahon NA, Yu SJ, Hubbard WC, et al. Expression of CYP1A1 gene in patients with lung cancer: evidence for cigarette smoke-induced gene expression in normal lung tissue and for altered gene regulation in primary pulmonary carcinomas. J Natl Cancer Inst. 1990;82:1333–9.

Nechay BR. Mechanisms of action of vanadium. Annu Rev Pharmacol Toxicol. 1984;24:501–24.

Oscar Aparicio JVG, Sekinger E, Yang A, Moqtaderi Z, Struhl K. Chromatin Immunoprecipitation for Determining the Association of Proteins with Specific Genomic Sequences In Vivo. Current Protocols in Molecular Biology. 2005; 69:21.3.16–7.

Puga A, Ma C, Marlowe JL. The aryl hydrocarbon receptor cross-talks with multiple signal transduction pathways. Biochem Pharmacol. 2009;77:713–22.

Rosenberg B, Vancamp L, Trosko JE, Mansour VH. Platinum compounds: a new class of potent antitumour agents. Nature. 1969;222:385–6.

Rushworth SA, Macewan DJ. HO-1 underlies resistance of AML cells to TNF-induced apoptosis. Blood. 2008;111:3793–801.

Samet JM, Graves LM, Quay J, Dailey LA, Devlin RB, Ghio AJ, et al. Activation of MAPKs in human bronchial epithelial cells exposed to metals. Am J Physiol. 1998;275:L551–8.

Santini RP, Myrand S, Elferink C, Reiners Jr JJ. Regulation of Cyp1a1 induction by dioxin as a function of cell cycle phase. J Pharmacol Exp Ther. 2001;299:718–28.

Schuetz EG, Schuetz JD, Thompson MT, Fisher RA, Madariage JR, Strom SC. Phenotypic variability in induction of P-glycoprotein mRNA by aromatic hydrocarbons in primary human hepatocytes. Mol Carcinog. 1995;12:61–5.

Skene SA, Dewhurst IC, Greenberg M. Polychlorinated dibenzo-p-dioxins and polychlorinated dibenzofurans: the risks to human health. A review. Hum Toxicol. 1989; 8:173–203.

Song MO, Freedman JH. Expression of copper-responsive genes in HepG2 cells. Mol Cell Biochem. 2005;279:141–7.

Stapleton HM, Baker JE. Comparing polybrominated diphenyl ether and polychlorinated biphenyl bioaccumulation in a food web in Grand Traverse Bay, Lake Michigan. Arch Environ Contam Toxicol. 2003;45:227–34.

Svensson BG, Nilsson A, Hansson M, Rappe C, Akesson B, Skerfving S. Exposure to dioxins and dibenzofurans through the consumption of fish. N Engl J Med. 1991; 324:8–12.

Vakharia DD, Liu N, Pause R, Fasco M, Bessette E, Zhang QY, et al. Polycyclic aromatic hydrocarbon/metal mixtures:

effect on PAH induction of CYP1A1 in human HEPG2 cells. Drug Metab Dispos. 2001;29:999–1006.

Wang X, Safe S. Development of an in vitro model for investigating the formation of the nuclear Ah receptor complex in mouse Hepa 1c1c7 cells. Arch Biochem Biophys. 1994;315:285–92.

Weber R, Gaus C, Tysklind M, Johnston P, Forter M, Hollert H, et al. Dioxin- and POP-contaminated sites–contemporary and future relevance and challenges: overview on background, aims and scope of the series. Environ Sci Pollut Res Int. 2008;15:363–93.

Westerink WM, Schoonen WG. Cytochrome P450 enzyme levels in HepG2 cells and cryopreserved primary human hepatocytes and their induction in HepG2 cells. Toxicol In Vitro. 2007;21:1581–91.